

RECEIVED BY TIC 21 1980

Presented at the American Society of Civil Engineers
Fall Convention and Exhibit, San Francisco, CA,
October 17-21, 1977

LBL-7007

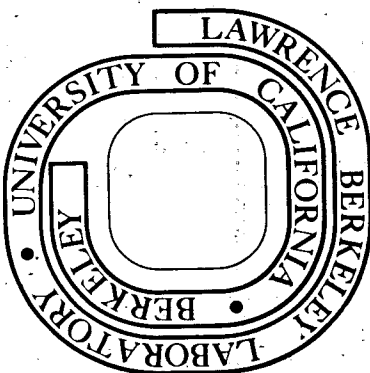
CONF-771027--3

MODELING SUBSIDENCE DUE TO GEOTHERMAL FLUID PRODUCTION

Marcelo J. Lippmann, T. N. Narasimhan,
and Paul A. Witherspoon

October 1977

Prepared for the U.S. Department of Energy
under Contract W-7405-ENG-48



MASTER

DISTRIBUTION OF THIS DOCUMENT IS UNLIMITED

DISCLAIMER

This report was prepared as an account of work sponsored by an agency of the United States Government. Neither the United States Government nor any agency Thereof, nor any of their employees, makes any warranty, express or implied, or assumes any legal liability or responsibility for the accuracy, completeness, or usefulness of any information, apparatus, product, or process disclosed, or represents that its use would not infringe privately owned rights. Reference herein to any specific commercial product, process, or service by trade name, trademark, manufacturer, or otherwise does not necessarily constitute or imply its endorsement, recommendation, or favoring by the United States Government or any agency thereof. The views and opinions of authors expressed herein do not necessarily state or reflect those of the United States Government or any agency thereof.

DISCLAIMER

Portions of this document may be illegible in electronic image products. Images are produced from the best available original document.

LEGAL NOTICE

This book was prepared as an account of work sponsored by an agency of the United States Government. Neither the United States Government nor any agency thereof, nor any of their employees, makes any warranty, express or implied, or assumes any legal liability or responsibility for the accuracy, completeness, or usefulness of any information, apparatus, product, or process disclosed, or represents that its use would not infringe privately owned rights. Reference herein to any specific commercial product, process, or service by trade name, trademark, manufacturer, or otherwise, does not necessarily constitute or imply its endorsement, recommendation, or favoring by the United States Government or any agency thereof. The views and opinions of authors expressed herein do not necessarily state or reflect those of the United States Government or any agency thereof.

MODELING SUBSIDENCE DUE TO GEOTHERMAL FLUID PRODUCTION

by

M. J. Lippmann, T. N. Narasimhan and P. A. Witherspoon

ABSTRACT

Currently, liquid dominated geothermal systems hold the maximum promise for exploiting geothermal energy in the United States. The principal characteristic of such systems is that most of the heat is transferred by flowing water, which also controls subsurface fluid pressures and stress changes. The reduction in pore pressures brought about by geothermal fluid extraction is potentially capable of causing appreciable deformation of the reservoir rocks leading to displacements at the land surface. In order to foresee the pattern and magnitude of potential ground displacements in and around producing liquid dominated geothermal fields, a numerical model has been developed. Conceptually, the simulator combines conductive and convective heat transfer in a general three dimensional heterogeneous porous medium with a one-dimensional deformation of the reservoir rocks. The capabilities of the model and its potential applicability to field cases are illustrated with examples considering the effects of temperature and pressure dependent properties, material heterogeneities and previous stress history.

Key words: Aquifers, compaction, computers, geothermal energy, pore-water pressures, subsidence.

DISCLAIMER

This book was prepared as an account of work sponsored by an agency of the United States Government. Neither the United States Government nor any agency thereof, nor any of their employees, makes any warranty, express or implied, or assumes any legal liability or responsibility for the accuracy, completeness, or usefulness of any information, apparatus, product, or process disclosed, or represents that its use would not infringe privately owned rights. Reference herein to any specific commercial product, process, or service by trade name, trademark, manufacturer, or otherwise, does not necessarily constitute or imply its endorsement, recommendation, or favoring by the United States Government or any agency thereof. The views and opinions of authors expressed herein do not necessarily state or reflect those of the United States Government or any agency thereof.

DISTRIBUTION OF THIS DOCUMENT IS UNLIMITED. *EB*

MODELING SUBSIDENCE DUE TO GEOTHERMAL FLUID PRODUCTION
Marcelo J. Lippmann¹, T. N. Narasimhan¹, Paul A. Witherspoon²

Introduction

The increasing dependence of the United States on imported fossil fuels and the uncertainty created by future rises in fuel prices has necessitated the search for new, less traditional domestic energy sources, such as geothermal energy. At the present time, geothermal steam is being used in the U. S. for electricity generation (The Geysers, California, 502 MWe) while geothermal water is used mainly for space heating (e.g., Boise, Idaho; Klamath Falls, Oregon). The exploitation of geothermal energy is expected to increase rapidly. For instance in 1979 the total installed capacity at The Geysers will rise to about 900 MWe (1). Also, new but smaller power plants are planned for other parts of the country. Nevertheless, the major increase is anticipated to occur in nonelectrical applications (i.e., space heating and cooling, agricultural and industrial uses) (2,3).

There exist different types of geothermal systems but currently only hydrothermal convection systems are being tapped for energy. These systems occur where circulating water and/or steam transfer heat from depth to the near-surface. A few of them may be vapor-dominated and produce saturated, or even supersaturated steam (e.g., The Geysers, California). But most hydrothermal systems deliver a mixture of hot water and steam at the surface. These are the so-called liquid-dominated systems (e.g., East Mesa, California; Raft River, Idaho) which are characterized at depth by the occurrence of saturated, porous or fractured rocks containing hot water which controls

¹Res. Eng., Lawrence Berkeley Laboratory, Univ. of California, Berkeley, Ca. 94720

²Assoc. Director, Lawrence Berkeley Laboratory, and Prof. Mat. Sci. and Min. Eng., Univ. of California, Berkeley, Ca. 94720

subsurface fluid pressures and stress changes (4). The results of resource assessment studies indicate that hot-water systems hold the maximum promise for developing geothermal energy in the United States (5).

A feature of these hot water systems is that they may experience significant reductions of pore fluid pressures as a consequence of large scale production of geothermal fluids. The decrease in pressures in the reservoir and surrounding water-saturated formations may cause appreciable rock deformations leading to displacements at the land surface. For example, significant surface deformations have already been observed over the Wairakei and Broadlands geothermal fields of New Zealand (6, 7) and are suspected to occur in Cerro Prieto, Mexico.

Because ground displacements may affect engineering structures related or unrelated to the operation of the geothermal field, it is important to be able to foretell the pattern and magnitude of the deformations that may result from fluid production so as to enable appropriate preventive or remedial actions. A number of mathematical models have been developed in the literature to predict ground deformations caused by reduction of pore pressures (8). Only a few of these are capable of simulating deformation of geothermal systems which, by their nature, are nonisothermal.

The results presented in the following pages illustrate the capabilities of a computer program developed at the Lawrence Berkeley Laboratory for solving heat and mass transfer accompanied by one-dimensional (vertical) deformation in saturated porous materials. The examples have been chosen to examine the significance of certain parameters on the deformation of geothermal systems.

Theory

The modeling of subsidence of a geothermal system due to fluid withdrawal can be divided into two parts: (1) simulation of reservoir deformation, and (2) simulation of overburden deformation. The reservoir (defined as the region

which releases fluid from storage to compensate for the fluid being withdrawn) deforms due to internally generated stresses resulting from changes in pore fluid pressures. The overburden (defined as the region which does not drain fluid from storage to compensate for the fluid withdrawn) deforms primarily due to the displacements induced at its interface with the deforming reservoir. The most general way of modeling the subsidence of such a system is to include the reservoir and the overburden within a single calculational model and to solve simultaneously the coupled fluid flow, heat flow and force equilibrium equations. Because of the large number of degrees of freedom and number of mesh points that may be involved in such computations this approach may prove to be impractical, especially for deep reservoirs.

On the other hand, a satisfactory solution may be obtained by using a dual reservoir-overburden model, in which the reservoir is assumed to deform according to Terzaghi's one-dimensional consolidation theory, while the overburden deforms due to arbitrary boundary loading in the form of displacements imposed at its interface with the reservoir. The assumption of one-dimensional (vertical) consolidation occurring in the reservoir seems justified for the following reason. Most liquid-dominated geothermal systems are comprised of alternating layers of permeable and less permeable materials. The permeable rocks are relatively rigid and tend to conduct fluid horizontally towards the producing wells, while the less permeable rocks are relatively more compressible and conduct fluids more or less vertically towards the permeable layers.

This paper is concerned only with the reservoir part of the dual reservoir-overburden model leading to the computation of the vertical displacements at the top of the reservoir. It is recognized that not all of this computed compaction will reach the ground surface, especially if the reservoir lies at a great depth. Some of the vertical deformation

may be attenuated as it is transmitted through the overburden and in addition, some horizontal displacements may be generated. The propagation of deformations through the overburden is currently under study and will be presented elsewhere (9).

Governing Equations

Based on the principles of conservation of mass, momentum and energy, several authors have developed the equations governing the heat and mass flow through porous media (10, 11, 12). For the case of a water-dominated geothermal system, the heat and mass flow equations can be expressed in an integral form as,

$$\frac{\partial}{\partial t} \int_V (\rho c)_M T dV = \int_S K_M \nabla T \cdot \bar{n} dS - \int_S \rho c_F \delta T \bar{v}_d \cdot \bar{n} dS + \int_V q dV \quad (1)$$

$$\frac{\partial}{\partial t} \int_V \frac{\rho}{1+e} \left(e \kappa + \frac{de}{d\sigma'} \right) P dV = \int_S \frac{k\rho}{\mu} (\nabla P - \rho \bar{g}) \cdot \bar{n} dS + \int_V Q dV \quad (2)$$

in which t = time; $(\rho c)_M$ = heat capacity per unit volume of the solid-fluid mixture; T = temperature; V = volume; K_M = thermal conductivity of the solid-fluid mixture; \bar{n} = outward unit normal on surface S ; ρ = fluid density; c_F = fluid specific heat capacity at constant volume; δT = difference between the mean temperature within volume element dV and that on the surface segment dS ; \bar{v}_d = Darcy fluid velocity; q = heat injection rate per unit volume; e = void ratio, κ = fluid compressibility; σ' = effective stress; P = pore pressure; k = intrinsic permeability; μ = viscosity; \bar{g} = acceleration due to gravity; Q = mass injection rate per unit volume. The energy and mass flow equations (Equations 1 and 2) are coupled through (a) the Darcy velocity (\bar{v}_d) used in the convection term of the energy equation and, (b) the temperature and/or pressure dependence of some parameters used in both equations.

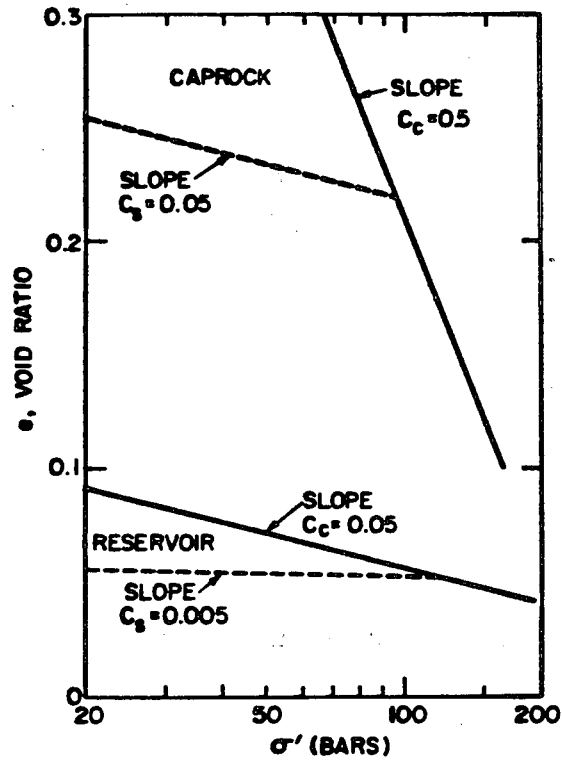
From the point of view of subsidence modeling the parameter $de/d\sigma'$

occurring in Equation 2 is of great interest. In the present model, this parameter is directly evaluated from the known functional dependence of e on σ' . The general, nonlinear, nonelastic deformation of the materials yielding water from storage as a result of pore pressure reduction may be conveniently described by "e-log σ' " curves (Figure 1). For each of these materials there is a virgin curve and, (if hysteresis is neglected), a series of parallel swelling-recompression curves. Thus, deformation is dependent on previous history.

Numerical Model

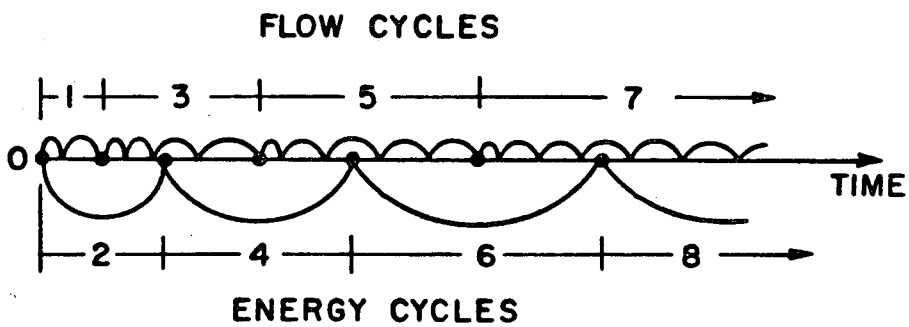
The numerical model "CCC" (for Conduction-Convection-Consolidation) developed at the Lawrence Berkeley Laboratory numerically solves the heat and mass flow equations and computes the vertical compaction of the simulated systems. This computer program which is a modification of codes SCHAFF (13) and TRUST (14) employs an Integrated Finite Difference Method (15) using an explicit-implicit iterative procedure to advance in time. Details of the algorithms are given elsewhere (13, 15, 16).

The coupled energy and mass flow equations are solved alternatively by interlacing them in time (see Figure 2). The flow equation solves for P , \bar{v}_d and e assuming that the temperature dependent properties remain constant. On the other hand, the energy equation computes T assuming that \bar{v}_d and the pressure dependent properties remain constant. Since pressure varies much faster than temperature, smaller time steps have to be taken in the flow cycles than in the energy cycles. Program CCC is designed to simulate one-, two- or three-dimensional heterogeneous, non-isothermal confined saturated porous systems. Hydraulic and thermal properties, including fluid density, may be linearly or nonlinearly dependent on pressure and/or temperature. As described above, the deformation parameters may in general be nonlinear and nonelastic. The code has been validated against different analytical and semianalytical



XBL 7611-7860

Figure 1. Plot of void ratio (e) versus effective stress (σ') for a hypothetical material



XBL 7611-7862

Figure 2. Interlacing of flow and energy calculations

solutions (17).

Illustrative Examples

Two groups of examples are presented below in order to demonstrate the capability of program CCC as well as to illustrate the effects of certain parameters used in the energy and mass transfer equations on reservoir compaction. The first group of problems relate to a three-layer geothermal system in which the producing aquifer is overlain by a caprock and underlain by bedrock. These problems have been chosen to illustrate the role of non-linear, nonelastic deformation parameters on reservoir compaction; the relation between subsidence history and reservoir pressure; and the importance of permeability changes due to changes in effective stress. The second group of problems relate to a two-layer system. The problems in this group have been chosen to examine the role of temperature dependence on different parameters entering into the governing equations and to study the effects of anisotropy and heterogeneity on spatial variation of reservoir compaction.

In the examples studied, fluid density may be either a function of temperature (Group 1) or may be a function of temperature and pressure (Group 2). In either case ρ is treated as a quadratic function of the dependent variable(s). Fluid viscosity, μ , and fluid heat capacity, c_F , are both functions of temperature (piecewise linear functions) while void ratio is a function of effective stress and previous stress history. All other parameters are assumed to be constant. Boundary conditions, including total stress distribution within the system do not change with time. Note that in the present calculations only the vertical deformations at the top of the reservoir-caprock system are computed. The transmission of such deformations through the overburden to the land surface is outside the scope of this paper.

Three-Layer System

The examples examined here serve to illustrate the dependence of system

deformation on the previous stress history of the materials. Also included here is an example studying the importance of the variation of intrinsic permeability as a consequence of effective stress changes induced by geothermal fluid extraction.

The hypothetical, three-layer system consists of a reservoir, a caprock and a bedrock, each 328 ft (100 m) thick. The caprock and bedrock are made up of one type of material, while the reservoir is of a second type (see Table 1). The system is axisymmetric, and has initial temperature and pressure conditions as given on Figure 3. The overburden (not shown on Figure 3) is 1328 ft (450 m) thick, and comprises materials with an average density of 156 lb/cu ft (2500 kg/m³). The boundary conditions used are as follows:

- (a) the upper and lower boundaries are impermeable and isothermal [455°F (235°C) and 509°F (265°C), respectively],
- (b) the radial boundary at a distance of 1246 ft (380 m) is a constant-pressure-and-temperature boundary for the reservoir and a closed boundary for the caprock and bedrock, and
- (c) the well located at the center of the system is pumped at a constant rate of 5.52×10^6 lb/day (2.5×10^6 kg/day).

The response of the three-layer system to 30 days of pumping is shown on Figures 4 and 5. Curves a and b correspond to overconsolidated materials with two different magnitudes of overconsolidation. Initially, at each point in the system the effective stress is smaller than the preconsolidation stress. Curve c describes the behavior of a normally consolidated system in which, at time zero, effective stress is equal to the preconsolidation stress at each point in the system.

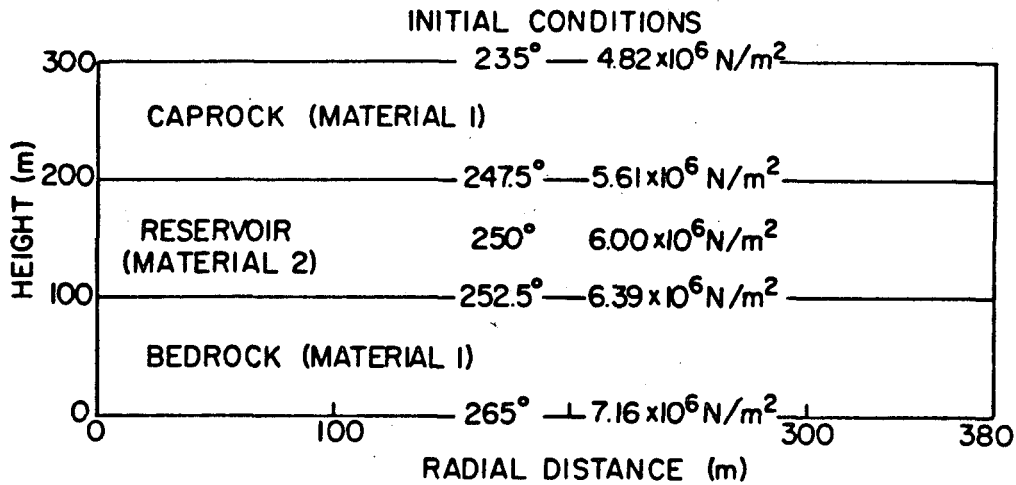
For curve a, the overconsolidation is equal to 102 psi (7×10^5 Pa). Because of this high value the deformation of the system is relatively small

TABLE 1. Material properties used in the examples

Property (1)	Three-Layer System		Two-Layer System	
	Caprock and Bedrock (2)	Reservoir (2)	Caprock (4)	Reservoir (5)
Heat capacity, in Btu lb ⁻¹ °F ⁻¹	0.222	0.232	0.222	0.232
Density, in lb/cu ft	168.6	165.4	168.6	165.4
Thermal conductivity (K _M), in Btu hr ⁻¹ ft ⁻¹ °F ⁻¹	0.669	1.672	0.609	1.605
Reference void ratio (e ₀)	0.250	0.111	0.250	0.053
Reference effective stress (σ ₀ '), in psi	1263.	1263.	2683.	2683.
Slope of virgin curve, in (log ₁₀ cycle) ⁻¹	0.5	0.05	0.5	0.05
Slope of swelling- recompression curve, in (log ₁₀ cycle) ⁻¹	0.01	0.01	0.05	0.005
Intrinsic permeability (k), in md.	0.03	30.0	0.10	50.0

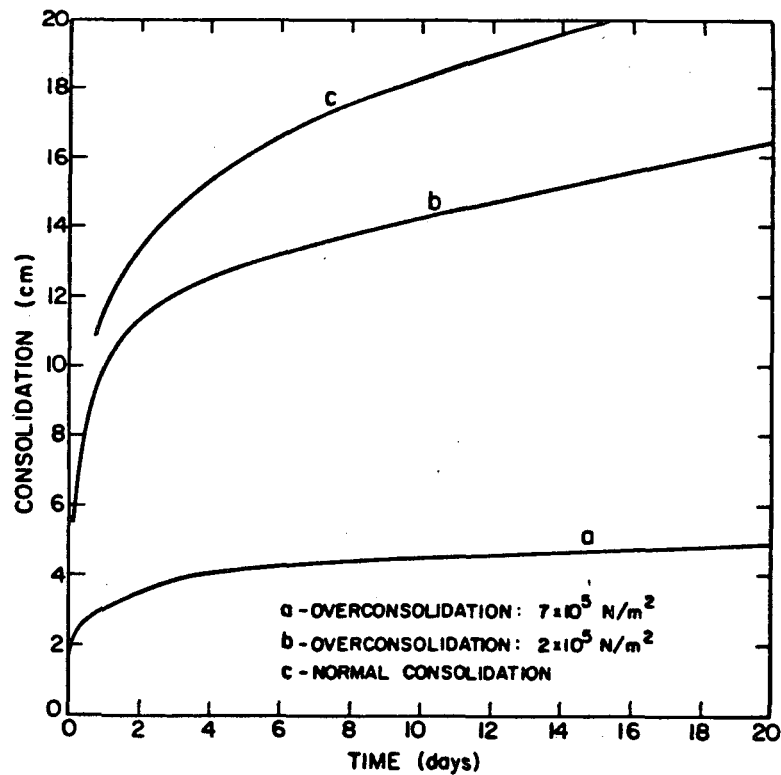
Note: 1 Btu lb⁻¹ °F⁻¹ = 4.186 J g⁻¹ °C⁻¹; 1 lb/cu ft = 16.02 kg m⁻³; 1 Btu hr⁻¹ ft⁻¹ °F⁻¹ = 1.731 W m⁻¹ °C⁻¹; 1 psi = 6895 Pa; 1 md = 9.86 x 10⁻¹⁶ m²

(Figure 4), with the stress-strain behavior of the materials following the recompression curves. Very little water is obtained from the compression of the rock skeleton. The compaction of the reservoir is significant at the beginning of the pumping period, but later, compaction of the caprock and bedrock becomes much more important (18). As can be seen in Figures 4 to 6 the system continues to consolidate even after the pressure has stabilized in the reservoir, because we are essentially concerned with a leaky aquifer system in which the more permeable aquifer goes to a steady-state while, in the less permeable caprock, the pressure transients move very slowly in the



XBL 773-5213

Figure 3. Geometry and initial conditions for the three-layer system. (Note: Temperature in degrees centigrades; 1 N/m² = 1 Pa = 1.45 x 10⁻⁴ psi; 1 m = 3.28 ft)



XBL 773-5209

Figure 4. Three-layer system: Plot of vertical compaction versus time under different initial overconsolidation conditions. (Note: 1 N/m² = 1 Pa = 1.45 x 10⁻⁴ psi; 1 cm = 0.0328 ft)

vertical direction, outward from the aquifer.

Curve c in Figures 4 and 5 relates to a system under normal consolidation, which deforms according to the much steeper virgin curves (see Figure 1 and Table 1), leading to relatively larger magnitudes of consolidation. Curve b corresponds to an intermediate case, with a lesser overconsolidation of only 29 psi (2×10^5 Pa). In this case, the materials deform at early times in accordance with the recompression curves. But, once effective stress exceeds the preconsolidation stress, the reduction in void ratio follows the virgin curves. This explains the intermediate behavior shown in Figures 4 and 5; curve b lies between curves a and c. Not only the computed compaction is different in each case, but also the response of the reservoir pressure is quite distinct (19). This is emphasized when the pressure is plotted against the amount of consolidation (Figure 5). This graph clearly reflects the effects of differences in overconsolidation values and in the slopes of the virgin and recompression curves. The flattening out of the curves at the top is related to the constant pressure assumed at the radial boundary. The behavior of the system with an overconsolidation equal to 29 psi (2×10^5 Pa) is quite interesting (see Figure 5, curve b). At the beginning it is identical to that of the system with a higher overconsolidation (curve a). When effective stress exceeds the preconsolidation value, the system deforms in a manner similar to that of the normally consolidated system (curve c). At this stage, curves b and c are essentially parallel. It is interesting to note that the response given by curve b (Figure 5) is similar to that observed in the Wairakei geothermal field of New Zealand, as shown in Figure 7, taken from Pritchett et al. (20).

The examples given above indicate the need to establish the deformation parameters of the various materials present in the field before one ventures to model subsidence in a given geothermal system. Laboratory techniques are

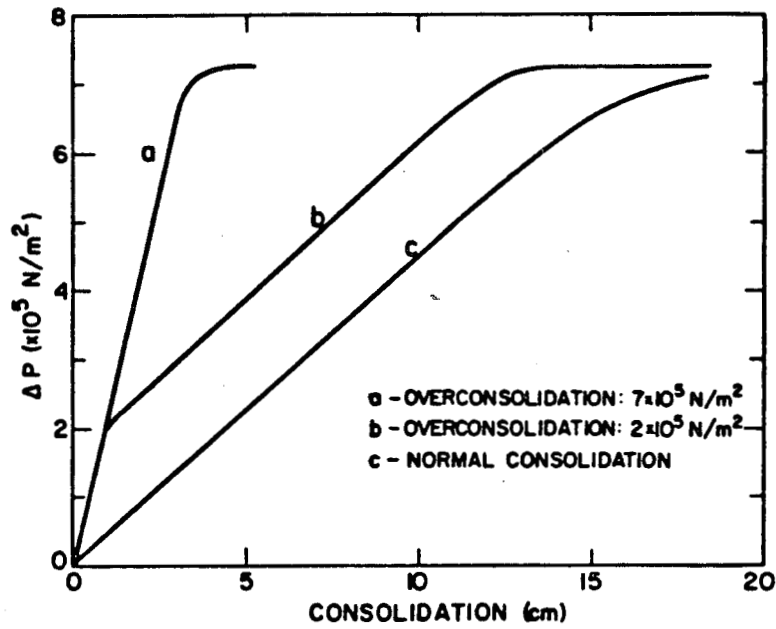


Figure 5. Three-layer system: Plot of reservoir pressure versus consolidation under different initial overconsolidation conditions. (Note: $1 \text{ N/m}^2 = 1 \text{ Pa} = 1.45 \times 10^{-4} \text{ psi}$; $1 \text{ cm} = 0.0328 \text{ ft}$)

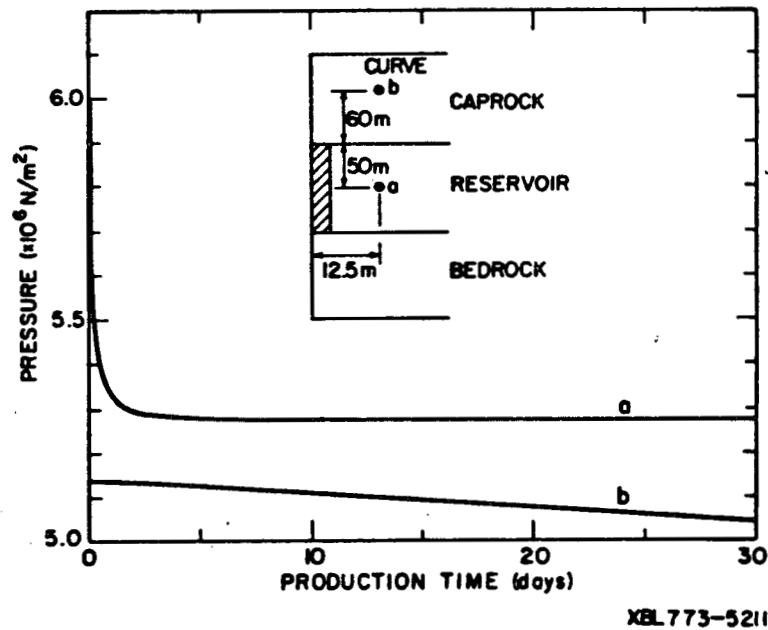
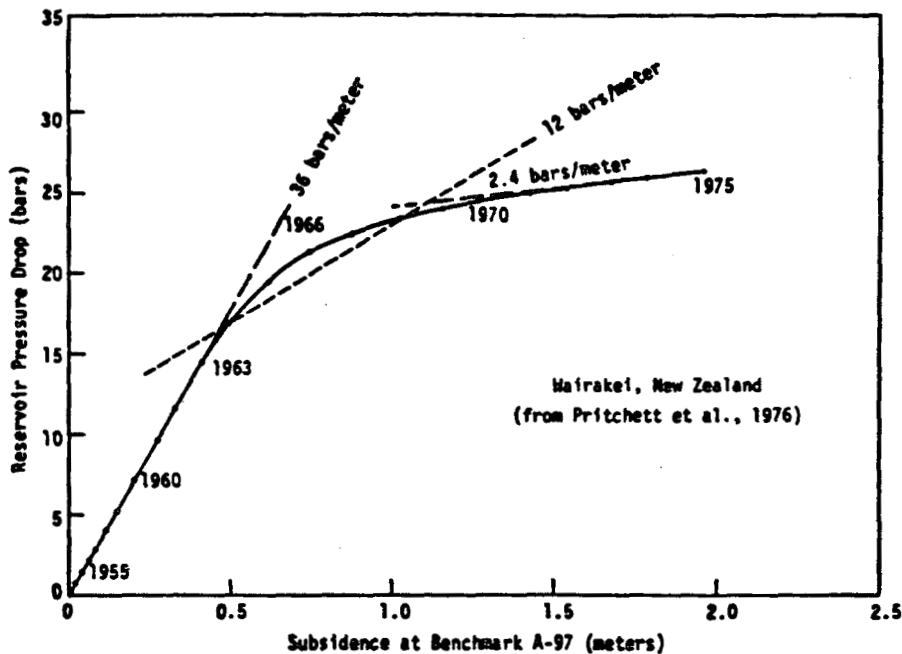


Figure 6. Three-layer system: Pressure change versus time in the reservoir and caprock for the case with overconsolidation = $7 \times 10^5 \text{ N/m}^2$. (Note $1 \text{ N/m}^2 = 1 \text{ Pa} = 1.45 \times 10^{-4} \text{ psi}$; $1 \text{ m} = 3.28 \text{ ft}$)



XBL 773-8173

Figure 7. Reservoir pressure drop versus subsidence at Wairakei, New Zealand (Note: 1 bar = 14.5 psi; 1 m = 3.28 ft)

available to measure the deformation properties of the rocks and their degree of overconsolidation. Field tests may establish the total stress and fluid pressures at different depths, as well as the prevailing boundary conditions. For a realistic field simulation, the aforesaid properties are of fundamental importance.

In considering deforming systems, a question which merits attention is that of the importance of the variation of intrinsic permeability due to changes in effective stress or, equivalently, void ratio. Computer program CCC has the ability to handle either piecewise linear or nonlinear dependence of k with e . One convenient way of handling the k versus e relation is to make the reasonable assumption (21, 22) that e is linearly related to $\log k$. Then, k can be conveniently evaluated from the relation,

$$k = k_0 \exp \frac{2.303 (e - e_0)}{C_k} \quad (3)$$

in which k_0 = reference intrinsic permeability; e_0 = reference void ratio; and C_k = slope of straight line on the e versus $\log k$ plot.

In order to study the effects of stress-dependent permeability on the deformation behavior of a given system, we consider the three-layer problem with normally consolidated materials (curve c in Figure 4). The permeability related parameters used in this case are summarized in Table 2.

The computations showed, as is to be expected, that the reduction of pore pressure caused by the fluid withdrawal resulted in decreased void ratios and thus, smaller intrinsic permeability values. The decreased permeability, in turn, led to somewhat larger pressure changes and small increases in the amount of consolidation, as compared with the constant permeability case. The difference in consolidation did not exceed 4 percent from those shown on Figure 4 (curve c).

TABLE 2. Three-layer system: Parameters governing variable intrinsic permeability

Parameter (1)	Caprock (2)	Reservoir (3)	Bedrock (4)
Reference intrinsic permeability (k_0), in md.	0.03	30.0	0.03
Reference void ratio (e_0)	.2765	.1111	.2263
Slope of straight line on e - $\log k$ plot (C_k), in $(\log_{10} \text{ cycle})^{-1}k$	0.05	0.05	0.05

(Note: 1 md = $9.862 \times 10^{-16} \text{ m}^2$)

The results of the computation are presented in Figures 8 and 9 and Table 3. The distribution of k values after 30 days of pumpage are given

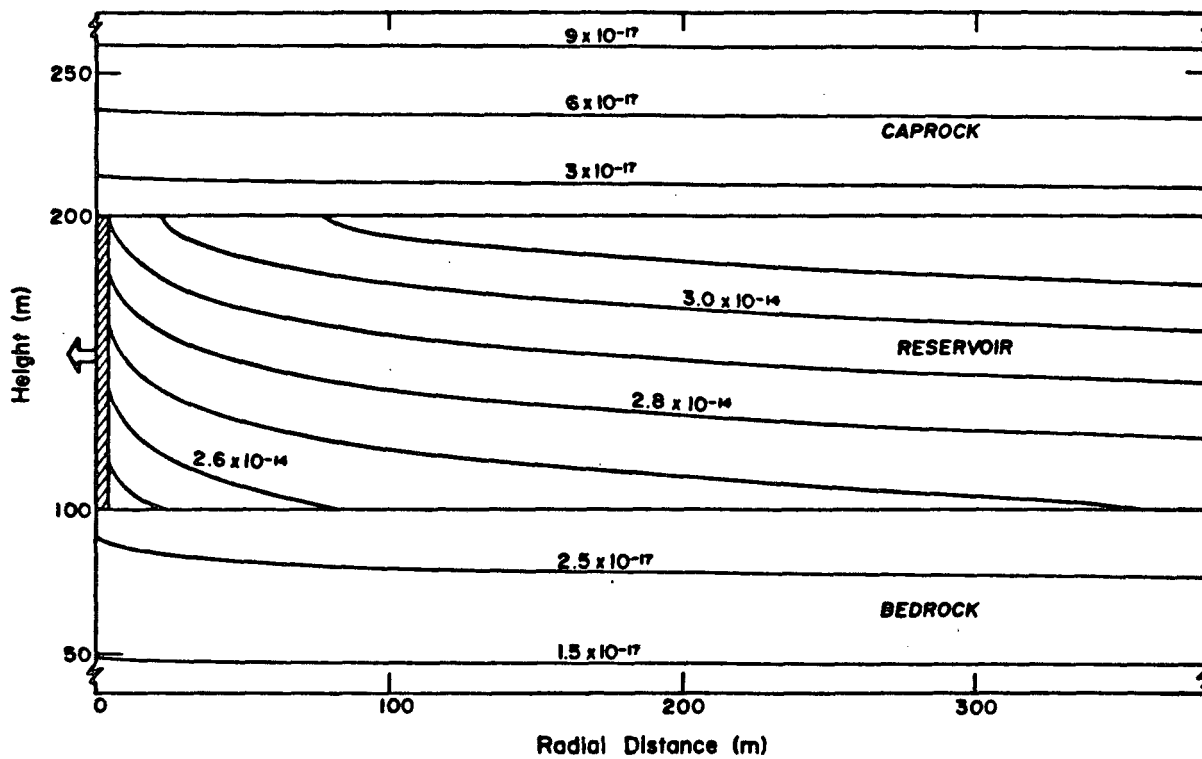


Figure 8. Three-layer system: Distribution of intrinsic permeability, in m^2 , after 30 days of pumping. (Note: $1 m^2 = 1.014 \times 10^{15}$ md).

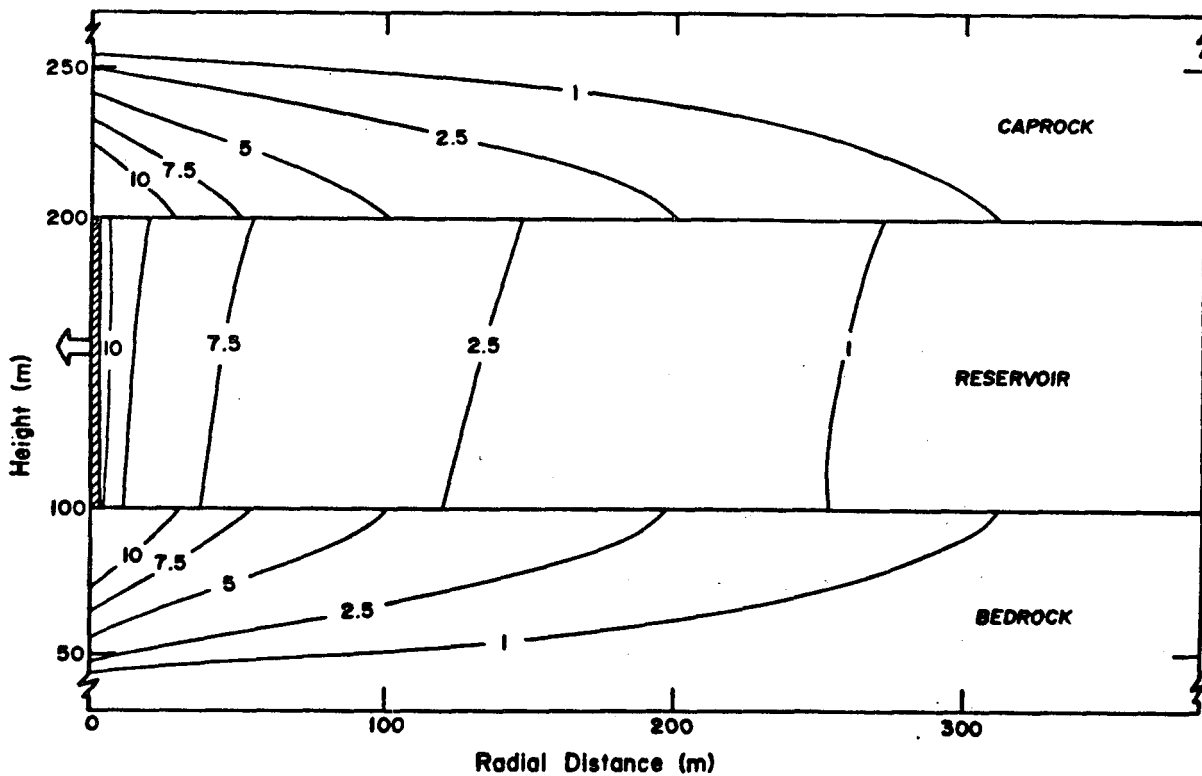


Figure 9. Three-layer system: Variation of intrinsic permeability in percent, after 30 days of pumping. (Note: $1 m = 3.28$ ft).

TABLE 3. Three-layer system: Effect of pumpage at two different locations in the system. Normally consolidated case with variable permeability.

Parameters (1)	Node 303 (2)	Node 703 (3)
Elevation above top of bedrock, in ft	295	32.8
Distance from well, in ft	41.0	41.0
<u>Pore Pressure (P), in psi</u>		
t = 0	824.6	914.5
t = 30 days	718.8	804.3
ΔP, in psi	-105.8	-110.2
<u>Effective Stress (σ'), in psi.</u>		
t = 0	1165.2	1359.4
t = 30 days	1271.0	1469.6
Δσ', in psi	105.8	110.2
<u>Void Ratio (e)</u>		
t = 0	.1128	.1095
t = 30 days	.1110	.1078
Δe	-.0018	-.0017
<u>Intrin. Permeab. (k), in md.</u>		
t = 0	32.5	27.9
t = 30 days	29.8	25.8
Δk, in md.	-2.7	-2.1

(Note: 1 ft = 0.305 m; 1 psi = 6895 Pa; 1 md = 9.86 x 10⁻¹⁶ m²)

in Figure 8. There is a drop in permeability values near the well and almost no change towards the radial constant-pressure boundary. The reduction in k, given in percent, is shown in Figure 9. A somewhat larger drop in permeability has occurred in the upper part of the reservoir, even though the pressure has decreased less than at the lower part (see Table 3); illustrating the effect of nonlinear deformation parameters. At the top of the effective stress is

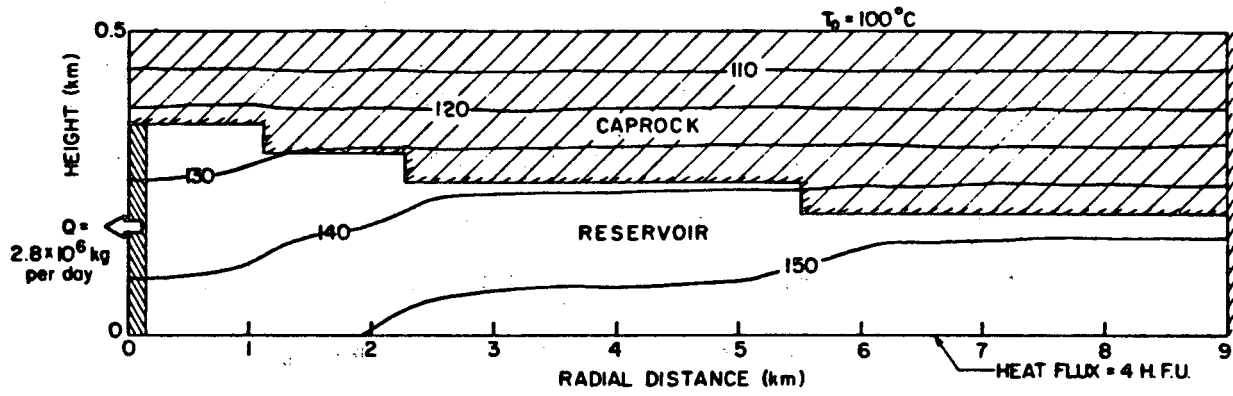
smaller than at the bottom, and a given change in pore pressure will result in a larger void ratio change than at the bottom (see Figure 1).

These preliminary results suggest that in deep systems where high effective stresses are generally present, and small void ratio changes occur, the variability of intrinsic permeability with changes in effective stress is likely to be small and hence can be conveniently neglected.

Two-Layer System

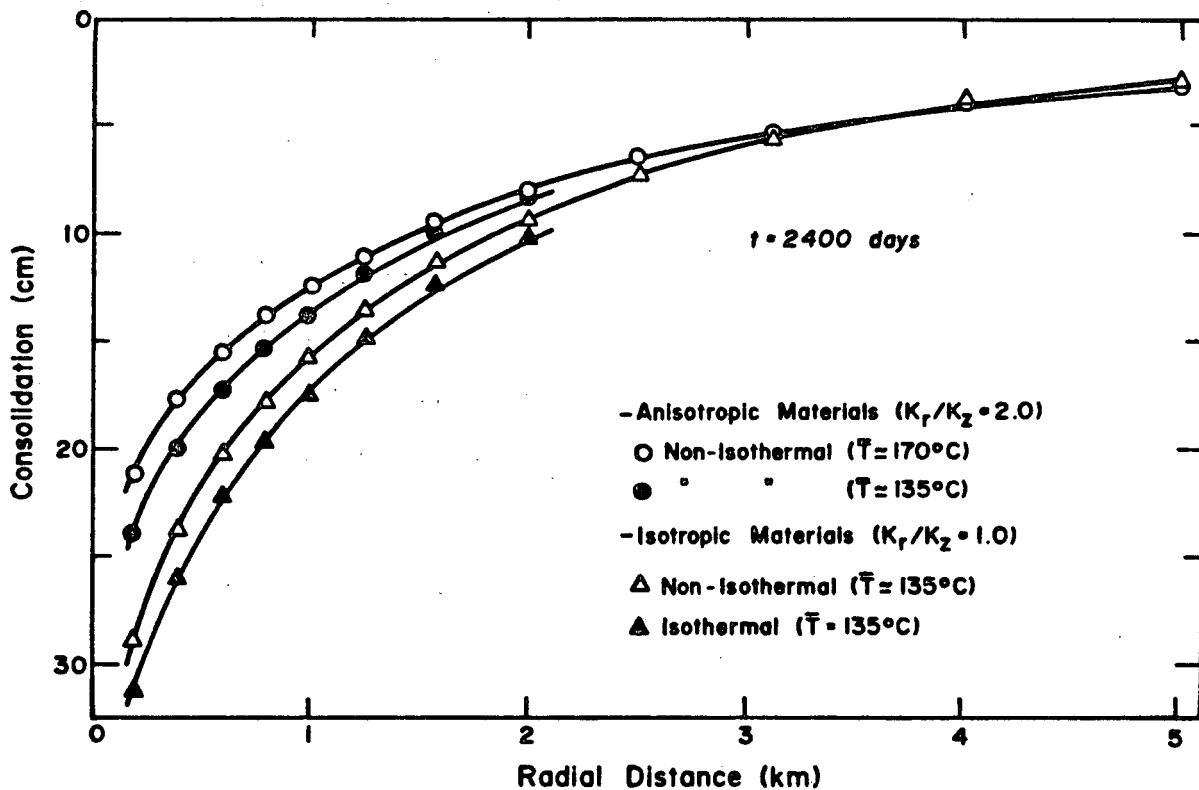
The examples in this group were chosen to illustrate the importance of analyzing compaction of a geothermal system using non-isothermal models, and to study the effects of temperature-dependent fluid properties, anisotropy and material heterogeneities. For this purpose a system with a caprock of variable thickness is considered. The initial and boundary conditions used are shown in Figure 10 and Table 1 lists the rock properties used. The lower boundary is impermeable with a constant heat influx of 5.31×10^{-2} Btu ft⁻² h⁻¹ (4×10^{-6} cal cm⁻² sec⁻¹). The upper boundary is impermeable and isothermal [212 °F (100°C)]. The radial boundary is closed to heat and fluid flow. A well located at the center of the radial system produces water at a constant rate of 6.18×10^6 lb/day (2.8×10^6 kg/day). The overburden (not shown) is 3279 ft (1000 m) thick and has an average density of 156 lb/cu ft (2500 kg m^{-3}).

The consolidation of the system after 2400 days of pumpage under different conditions is shown on Figure 11. In the case of isotropic materials, the isothermal model has yielded higher consolidation than the non-isothermal one. This difference in behavior is essentially due to the constant average properties assigned to the isothermal system, while the non-isothermal one has temperature-dependent fluid properties. The variability of viscosity with temperature appears to have considerable role in governing the consolidation of the non-isothermal system (18).



XBL 7611-7870

Figure 10. Two-layer system: Geometry, initial and boundary conditions. (Note: 1 km = 0.621 mi; 1 kg/day = 2.21 lb/day; 1 H.F.U. = 1.33×10^{-2} Btu ft⁻² h⁻¹).



XBL 778-2859

Figure 11. Two-layer system: Effect of temperature and anisotropy on consolidation (Note: 1 km = 0.621 mi; 1 cm = 0.0328 ft).

Also on Figure 11 are shown two examples with anisotropic materials. In these, the radial intrinsic permeability (k) and thermal conductivity (K) are the same as in the isotropic case, but the vertical properties are reduced by a half. In one case the thermal boundary conditions are kept unchanged (see Figure 10). The decrease in vertical conductivity results in an increase in vertical thermal gradient which in turn leads to an increase in average system temperature [from 275°F (135°C) to 338°F (170°C)]. In the other case, the thermal recharge through the lower boundary was reduced by a half to keep the same average temperature as in the isotropic examples [275°F (135°C)].

From an analysis of the four curves shown on Figure 11 it can be concluded that:

- (a) the use of isothermal models to simulate geothermal systems may result in predicting somewhat larger and conservative consolidation values than in the non-isothermal case.
- (b) higher temperatures (and lower fluid viscosities) in the system may reduce the magnitude of consolidation near the pumped well.
- (c) the presence of anisotropic materials tend to reduce the consolidation near the well, while slightly increasing it away from it (the curves on Figure 11 cross each other at large radial distance from the well).

The effect of anisotropy on the consolidation pattern within the system is further illustrated in Figure 12. In the isotropic case the percentage of total consolidation which occurs in the caprock is significantly larger than in the anisotropic case. This is explained by the lower vertical permeabilities in the latter example. Since the mass flow in the caprock is essentially vertical towards the reservoir, a reduction in vertical permeability diminishes the release of fluids from the caprock, thus resulting in smaller pressure drops

and lower caprock compaction.

The effect of geological heterogeneities is further explored by introducing a lense of caprock material within the reservoir (Figure 13). Other conditions remain the same as in Figure 10. As can be seen from Figure 13, the presence of a compressible lense within the reservoir affects the tortuosity of flow path and the pressure distribution near the well leading to a dramatic change in the profile of the subsidence bowl. Note that the maximum subsidence of about 15 in (38 cm) occurs approximately 0.25 mi (0.4 km) away from the producing well. This simplistic model may perhaps provide a clue to understanding the interesting subsidence pattern at Wairakei [(6) and Figure 14], where the subsidence bowl is observed to be offset approximately 1 mile (1.61 km) east northeast of the main producing area. In the light of the results presented in Figure 13 one may conjecture that the disposition of the subsidence bowl at Wairakei is related to the presence of relatively large thickness of highly compressible materials below the region of the subsidence bowl.

Concluding Remarks

The present work has shown that the one-dimensional deformation model, in conjunction with the multi-dimensional heat-mass transfer simulator is of considerable utility in studying deformation of geothermal reservoirs. Although the model does not carry out stress-strain calculations in a general multi-dimensional form, the simplified assumptions used in the present model appear justified due to the fact that many geothermal systems (e.g. Wairakei, New Zealand, Imperial Valley, California) may be composed of alternating layers of permeable and poorly permeable (but compressible) materials and the fact that the internal loading on the rock skeleton induced by pore pressure withdrawal is hydrostatic and affects mainly the diagonal components of the stress tensor. An added advantage of the present approach is

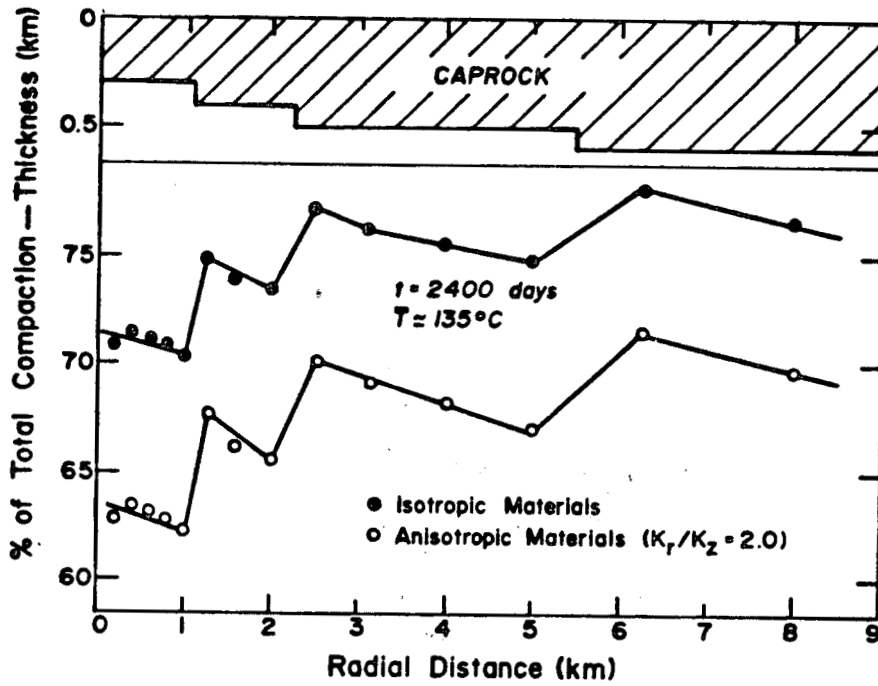


Figure 12. Two-layer system: Effect of anisotropy on percent of consolidation occurring in the caprock. (Note: 1 km = 0.621 mi).

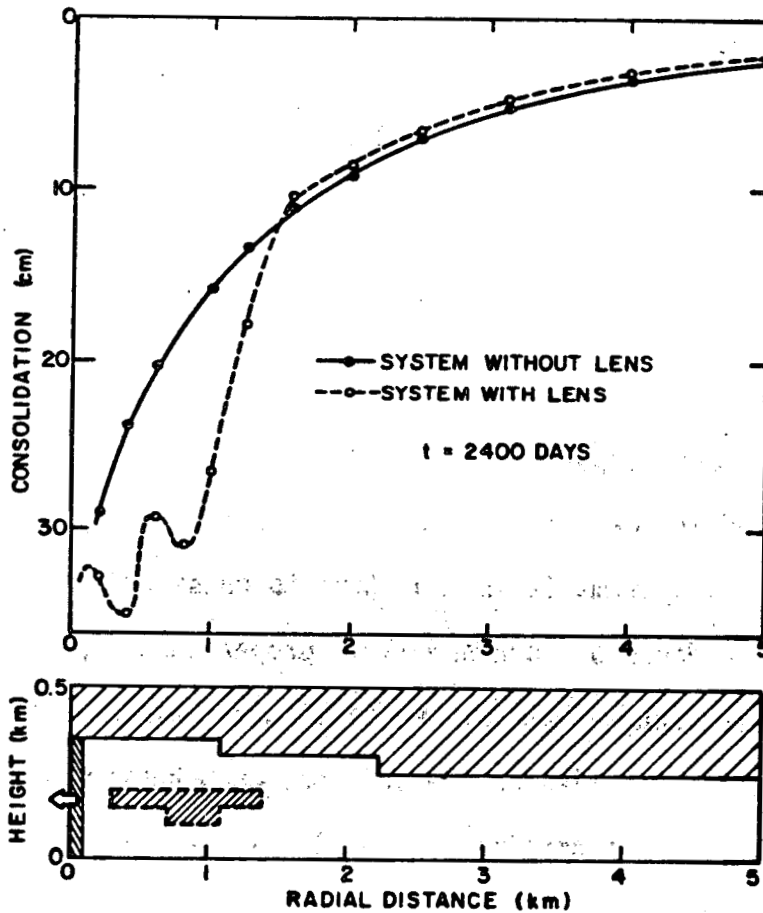


Figure 13. Effect of an heterogeneity on the consolidation profile of the two-layer system. (Note: 1 km = 0.621 mi; 1 cm = 0.0328 ft).

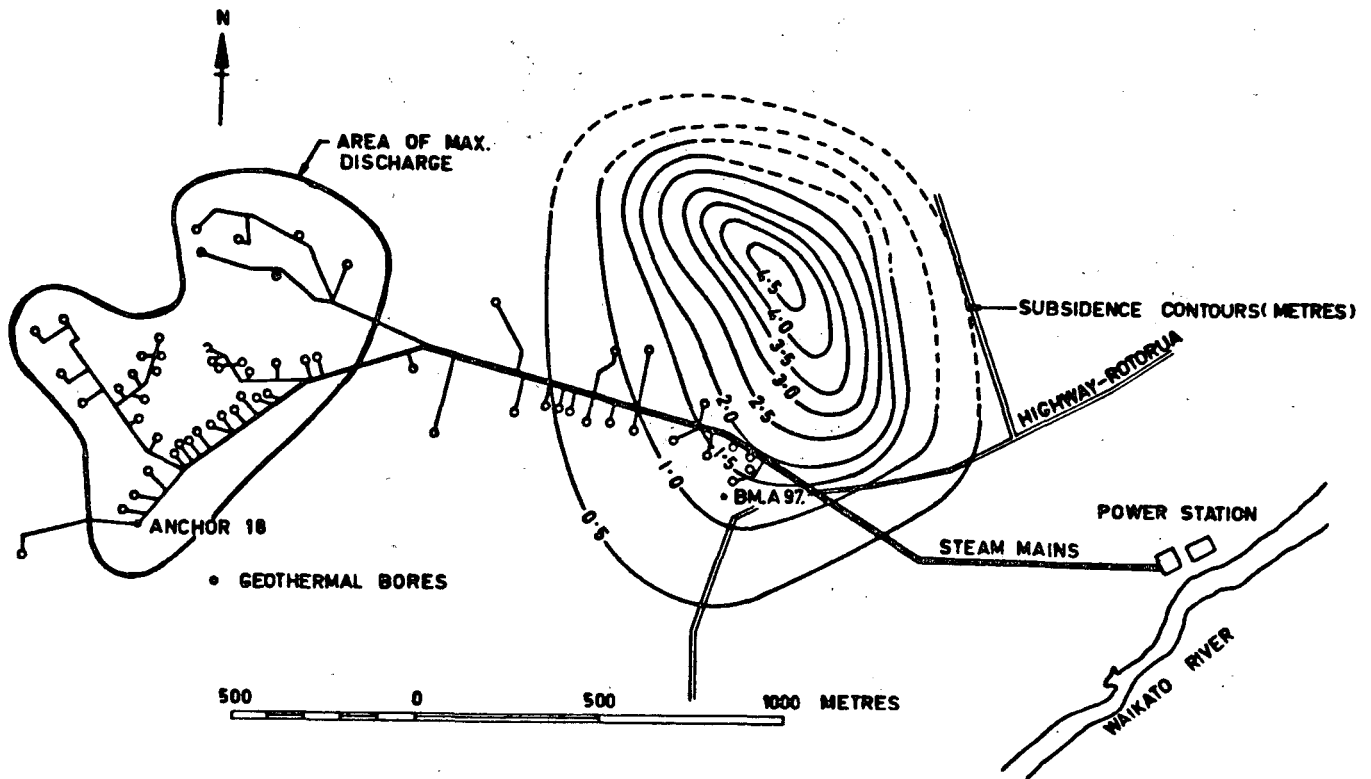


Figure 14. Total subsidence at Wairakei geothermal field, New Zealand, 1964 to 1974. Taken from Stilwell et al. (1975). (Note: 1 m = 3.28 ft).

that the deformation computation is intrinsically coupled with the fluid flow calculation without resorting to an independent solution of the stress-strain equation. It is well known that the additional set of equations related to stress-strain greatly increase computational effort and cost.

The examples presented indicate that in order to realistically simulate the compaction of geothermal systems it is important to consider the temperature (and/or pressure) dependence of rock and fluid properties, especially viscosity. Also the significant effects of previous stress history of the materials and those of heterogeneities on the deformation behavior of these systems has been illustrated. The preliminary results suggest that for deep reservoirs the effect of intrinsic permeability variation with void ratio changes, may only be of secondary significance.

Acknowledgement

This work was done with support from the U. S. Energy Research and Development Administration under Contract W-7405-ENG-48.

Appendix I. References

1. Weres, O., Tsao, K., and Wood, B., "Resource, Technology and Environment at the Geysers," Report LBL-5231, Lawrence Berkeley Laboratory, University of California, Berkeley, California, July 1977.
2. Howard, J. H., "Principal Conclusions of the Committee on the Challenges of Modern Society Non-electrical Applications Project," Proceedings of the Second United Symposium on the Development and Use of Geothermal Resources, Vol. 3, May 1975, pp. 2127-2139.
3. Reistad, G. M., "Potential for Nonelectrical Applications of Geothermal Energy and their Place in the National Economy," Proceedings of the Second United Nations Symposium on the Development and Use of Geothermal Resources, Vol. 3, May 1975, pp. 2155-2164.
4. Renner, J. L., White, D. E., and Williams, D. L., "Hydrothermal Convection Systems," Geological Survey Circular 726, 1975, pp. 5-57.
5. White, D. F. and Williams, D. L., "Assessment of Geothermal Resources of the United States - 1975, Summary and Conclusions," Geological Survey Circular 726, 1975, pp. 147-155.
6. Stilwell, W. B., Hall, W. K., and Tawhai, J., "Ground Movement in New Zealand Geothermal Fields," Proceedings of the Second United Nations Symposium on the Development and Use of Geothermal Resources, Vol. 2, May 1975, pp. 1427-1434.
7. Otway, P. M., "Report on Results on Precise and Tilt-Levelling: Broadlands ReInjection Project, 1968-76," presented at the August 29 - September 3, 1976 International Conference on the Geothermal Reservoir, held at Wairakei, New Zealand.
8. Finnemore, J. E. and Gillan, M. L., "Compaction Processes and Mathematical Models of Land Subsidence in Geothermal Areas", Proceedings of the Second Symposium on Land Subsidence - 1976 at Anaheim, International Association of Hydrological Sciences (in press).
9. Narasimhan, T. N., et al., "A Dual Reservoir-Overburden Model for Simulating Land Subsidence due to Fluid Withdrawal from Deep Systems," to be presented at the January 15-20, 1978, Engineering Foundation Meeting, to be held at Pensacola Beach, Florida.
10. Pritchett, J. W., et al., "Geohydrological Environmental Effects of Geothermal Power Production. Phase I," Report SSS-R-75-2733, Systems, Science and Software, La Jolla, California, September 1975.

11. Faust, C. R., and Mercer, J. W., "Theoretical Analysis of Fluid Flow and Energy Transport in Hydrothermal Systems," Open-File Report 77-60, U. S. Geological Survey, Reston, Virginia, 1977.
12. Witherspoon, P. A., et al., "Modeling Geothermal Systems," Atti dei Convegni Lincei, Accademia Nazionale dei Lincei, Vol. 30, 1977, pp. 173-221.
13. Sorey, M. L., "Numerical Modeling of Liquid Geothermal Systems," Open-File Report 75-613, U. S. Geological Survey, Menlo Park, California, 1975.
14. Narasimhan, T. N., "A Unified Numerical Model for Saturated-Unsaturated Groundwater Flow," thesis presented to the University of California, at Berkeley, California, in 1975, in partial fulfillment of the requirements for the degree of Doctor of Philosophy.
15. Narasimhan, T. N. and Witherspoon, P. A., "An Integrated Finite Difference Method for Analyzing Fluid Flow in Porous Media," Water Resources Research, Vol. 12, No. 1, February 1976, pp. 57-64.
16. Edwards, A. L., "TRUMP: A Computer Program for Transient and Steady State Temperature Distribution in Multidimensional Systems," Report UCRL-14754, Rev. 3, Lawrence Livermore Laboratory, Livermore, California, September 1972.
17. Tsang, C. F., et al., "Numerical Modeling of Cyclic Storage of Hot Water in Aquifers," presented at the December 6-10, 1976, American Geophysical Union Fall Annual Meeting, held at San Francisco, California (Lawrence Berkeley Laboratory Report LBL-5929).
18. Lippmann, M. J., Narasimhan, T. N. and Witherspoon, P. A., "Numerical Simulation of Reservoir Compaction in Liquid Dominated Geothermal Systems," Proceedings of the Second Symposium on Land Subsidence - 1976 at Anaheim, International Association of Hydrological Sciences (in press).
19. Lippmann, M. J., Tsang, C. F. and P. A. Witherspoon, "Analysis of the Response of Geothermal Reservoirs under Injection and Production Procedures," presented at the April 13-15, 1977, 47th Annual California Regional Meeting of the Society of Petroleum Engineers of AIME, held in Bakersfield, California (preprint SPE 6537).
20. Pritchett, J. W., Garg, S. K., and Brownell, D. H., "Numerical Simulation of Production and Subsidence at Wairakei, New Zealand," Report SGP-TR-20, Stanford Geothermal Program, Stanford, California, December 1976, pp. 310-323.
21. Lamb, T. W. and Whitman, R. V., Soil Mechanics, John Wiley and Sons, Inc., New York, New York, 1969, pp. 281-292.
22. Narasimhan, T. N. and Witherspoon, P. A., "Numerical Model for Saturated-Unsaturated Flow in Deformable Porous Media - I. Theory," Water Resources Research, Vol. 13, No. 3, June 1977, pp. 657-664.

Appendix II. Notation

The following symbols are used in this paper:

C_c = slope of virgin curve in "e-log σ' plot";

C_k = slope of straight line in "e-log k plot";

C_s = slope of swelling-compression curve in "e-log σ' plot";

c_F = fluid specific heat capacity at constant volume;

e = void ratio;

\bar{g} = acceleration due to gravity;

K_M = thermal conductivity of solid-fluid mixture;

k = intrinsic permeability;

\bar{n} = outward unit normal on surface S ;

P = pore-fluid pressure;

Q = mass injection rate per unit volume;

q = energy injection rate per unit volume;

S = surface;

T = temperature;

t = time;

V = volume;

\bar{v}_d = Darcy fluid velocity;

δT = difference between the mean temperature within volume element dV and that on the surface segment dS ;

κ = fluid compressibility;

μ = fluid viscosity;

ρ = fluid density;

$(\rho c)_M$ = heat capacity per unit volume of the solid-fluid mixture; and

σ' = effective stress

Subscripts

— = average

Superscripts

o = reference quantity